



Carbon-coated Cu-Co bimetallic nanoparticles as selective and recyclable catalysts for production of biofuel 2,5-dimethylfuran

Bingfeng Chen, Fengbo Li*, Zhijun Huang, Guoqing Yuan*

Beijing National Laboratory of Molecular Science, Key Laboratory of Green Printing, Institute of Chemistry, Chinese Academy of Sciences, Beijing 100190, PR China

ARTICLE INFO

Article history:

Received 16 February 2016

Received in revised form 6 June 2016

Accepted 4 July 2016

Available online 6 July 2016

Keywords:

Nanoparticles
Bimetallic catalysts
Synergistic effect
Hydrogenolysis
Biofuel

ABSTRACT

Cu-Co bimetallic nanoparticles coated with carbon layers have been developed through direct heating treatment of bimetallic oxide precursors incipiently deposited with polyethylene glycol. The as-synthesized nanocatalyst performs excellently in chemoselective hydrogenolysis of 5-hydroxymethylfurfural to 2,5-dimethylfuran. The Co-based catalysts exhibit higher performance than Cu-based catalysts. Cu-Co@C (Cu: Co = 1:3) shows the highest yield of 2,5-dimethylfuran (99.4%). Bimetallic nanocatalysts are detailedly characterized by transmission electron microscopy (TEM), X-ray diffraction (XRD) and X-ray photoelectron spectroscopy (XPS). The bimetallic nanoparticles are entrapped by carbon shells that can protect them from oxidation and deactivation. The catalytic activity and selectivity are kept constant in a six-run recycling test. The synergistic effect between two metal components is helpful to enhance catalytic performance.

© 2016 Elsevier B.V. All rights reserved.

1. Introduction

Biomass resources are abundant and renewable carbon feedstocks for the production of biofuel components [1,2]. These potential carbon-neutral fuels could reduce energy dependence on fossil fuels and abate the build-up of CO₂ in the environment [3]. Some platform molecules can be derived from cellulose, such as 2,5-dimethylfuran (DMF), 2-methylfuran (2-MF), 5-ethoxymethylfurfural (EMF), ethyl levulinate (EL), γ -valerolactone (GVL), and pentyl valerate (PV) [4–6]. These chemicals have great potentials in being used as biofuel components. DMF is the most promising one with high energy density, high octane number, and proper boiling point [7,8]. DMF-blended gasoline has shown efficient application in a single-cylinder gasoline direct-injection gasoline engine [9]. Through the cycloaddition with ethylene, DMF can be converted to *p*-xylene [10,11].

DMF can be produced through selective hydrodeoxygenation of a platform molecule from cellulose (5-hydroxymethylfurfural, HMF) [12]. HMF is a chemically active molecule with several functional groups. During hydrogenation or hydrogenolysis of HMF, there are many competitive reaction routes such as partial hydrogenation, total hydrogenation, ring hydrogenation, ring-opening, and

hydrodeoxygenation [13]. The key issue is the development of highly selective hydrodeoxygenation catalysts for converting HMF to DMF. Dumesic et al. have reported that the Cu-Ru/C catalyst gave a medium yield of DMF (76–79%) from fructose by a biphasic process [4]. Hydrogenolysis of HMF to DMF over the combined ZnCl₂-Pd/C catalyst has claimed a high yield of 85% [14]. Ru-Co₃O₄ and Pt-Co bimetallic nanoparticles encapsulated in carbon nanospheres were reported to be highly efficient catalyst for DMF production from HMF with high yields above 90% [15,16]. Through transfer hydrogenation reaction, HMF can also be converted to DMF over noble metal catalysts/hydrogen donors, such as Pd/C with formic acid [3], Pd/Fe₂O₃ with 2-propanol [17], and Ru/C with 2-propanol [18].

Precious metals (Pt, Pd, Rh, Ru, Ir, Os, Re) in most cases show high activity and selectivity in catalytic hydrogenation or hydrogenolysis under mild conditions. However, they are very expensive because of the low abundance and substantial costs are high during the required recovery and recycle processes [19–25]. Base metals (Ni, Co, Cu, Fe) are the preferred catalysts for hydrotreating many function groups under higher reaction temperature and hydrogen pressure [26–29]. But they show poor selectivity and recyclability [30–33]. Great efforts have been put into replacing precious metal catalysts and this gives an impetus to developing base metal catalysts with improved selectivity and stability [34,35]. The development of nanosciences offers specific solutions to improve catalytic performances through harnessing nanostruc-

* Corresponding authors.

E-mail addresses: libf@iccas.ac.cn (F. Li), yuangq@iccas.ac.cn (G. Yuan).

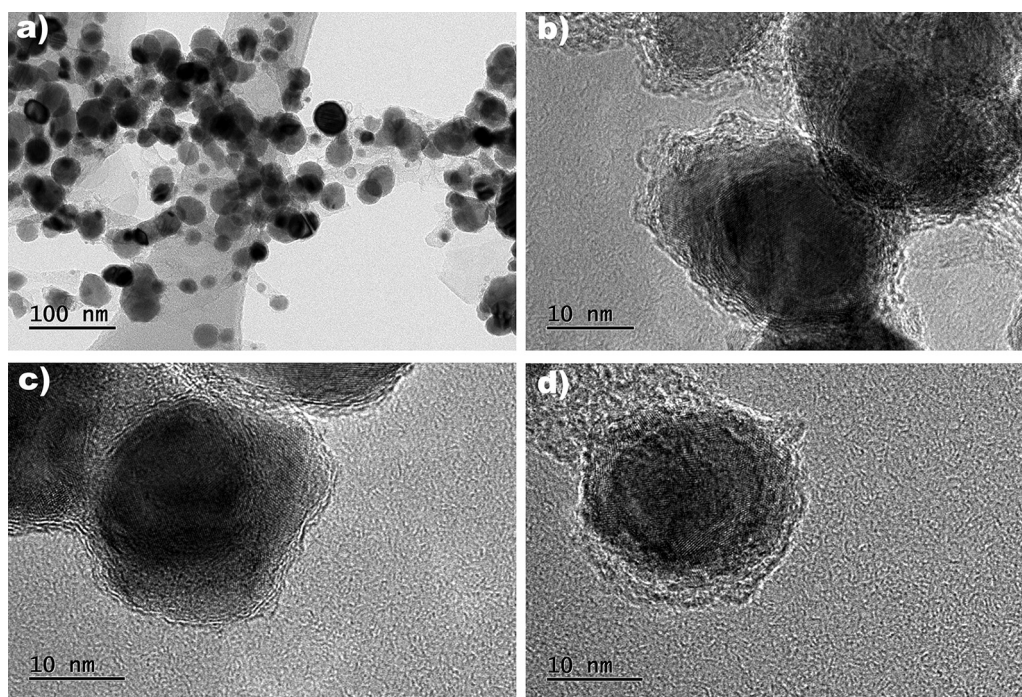


Fig. 1. (a) TEM image of Cu-Co@Carbon nanoparticles at low magnification. (b–d) TEM images of the selected single bimetallic nanoparticle.

tured or nanoscale materials as the catalysts. Supported metal nanoparticles and metal species dispersed over nanomaterials are general nanocatalysts that afford specific properties from quantum size effect. However, nanoparticles of base metals (Ni, Co, Cu, Fe) are not air-stable and fast deactivation takes place under the practical operation [36–38].

HMF hydrogenolysis catalysts based on base metals have been attempted in many recent researches. Ni-W₂C bi-component catalysts supported over activated carbon have been reported to be efficient catalysts for converting HMF to DMF with a yield of 96% [39]. Copper-based catalysts show activity in a switchable synthesis of DMF and 2, 5-furandimethanol from HMF [40]. Ni-Fe alloy species supported over carbon nanotube give a DMF yield of 91.3% during catalyzing hydrogenolysis of HMF [41]. Copper-zinc nano-alloy catalyst has a combined yield of 97% of DMF and 2, 5-dimethyltetrahydrofuran (DMTHF) [42].

In this work, the precursors of carbon-coated bimetallic nanoparticles were prepared by a solvothermal method. The catalytic materials were obtained through further heating treatment of the precursors in argon flow. The deposition of polyethylene glycol over the precursors acts as the sources of carbon layers and the reductant for metal species. The formation of zero-valent metal centers and their synergistic effects with cobalt oxide species endow the supported nanoparticles with unexpected selectivity and activity in hydrogenolysis of HMF. Coating of carbon layers leads to excellent recyclability.

2. Experimental

2.1. Materials

5-Hydroxymethylfurfural (99.0%) and 2,5-bis(hydroxymethyl) furan (98.0%) were purchased from Acros Organics. Pd/C (Pd: 10 wt.%), Pt/C (Pt: 5 wt.%), Ru/C (Ru: 5 wt.%), Rh/C (Rh: 5 wt.%) and Raney Ni were obtained from Alfa Aesar. Co(NO₃)₂·6H₂O, Cu(NO₃)₂·2H₂O, Ni(NO₃)₂·6H₂O, Fe(NO₃)₃·9H₂O, ZnCl₂, AgNO₃

were purchased from Sinopharm Chemical Reagent Co. Ltd (Shanghai, China).

2.2. Preparation of catalytic materials

Carbon-coated Cu-Co bimetallic nanoparticles were prepared by the modified Pechini-type sol-gel method. Co(NO₃)₂·6H₂O and Cu(NO₃)₂·2H₂O were added to water (20 ml, total metal amount: 6.25 mmol). The mole ratio of Cu to Co can be adjusted from 3:1 to 1:5. Then tartaric acid (TA, 12.5 mmol) was added to the mixtures. Glycerol/water mixture (v/v = 4: 1, 60 ml) and polyethylene glycol (average MW: 6000, 5.0 g) were added. The mixtures were further dispersed under sonication for 1.0 h, and transferred to a hydrothermal reaction vessel, and then heated to 150 °C for 13 h. The solid materials were collected by centrifugal separation, and washed with ethanol for three times, and dried at 100 °C overnight. Carbon-coated Cu-Co bimetallic nanoparticle catalysts were prepared by treating the precursors at 800 °C in argon flow for 2.0 h.

Carbon-coated Cu-Ni, Cu-Fe, Cu-Zn, Zn-Co, Ag-Co and Ni-Co bimetallic nanoparticle catalysts were prepared through the same procedure as carbon-coated Cu-Co bimetallic nanoparticles. Selected metal precursor salts were changed according to the target materials.

2.3. Characterization of catalytic materials

Transmission electron microscopy (TEM) was performed on a JEOL 2010 TEM equipped with an attachment for local energy dispersion analysis (EDX). The accelerating voltage was 200 kV, and the spot size was 1 nm. High-angle annular dark field scanning transmission microscopy (HAADF-STEM) was performed on the carbon-coated Cu-Co bimetallic nanoparticle catalysts with JEOL JEM-2100F microscope in a scanning transmission electron microscopy (STEM) mode operated at 200 kV.

Powder X-ray diffraction (XRD) patterns were measured on a Rigaku Rotaflex diffractometer equipped with a rotating anode and a Cu-Kα radiation source (40 kV, 200 MA; λ = 1.54056 Å). XPS data were obtained with an ESCALab220i-XL electron spectrometer

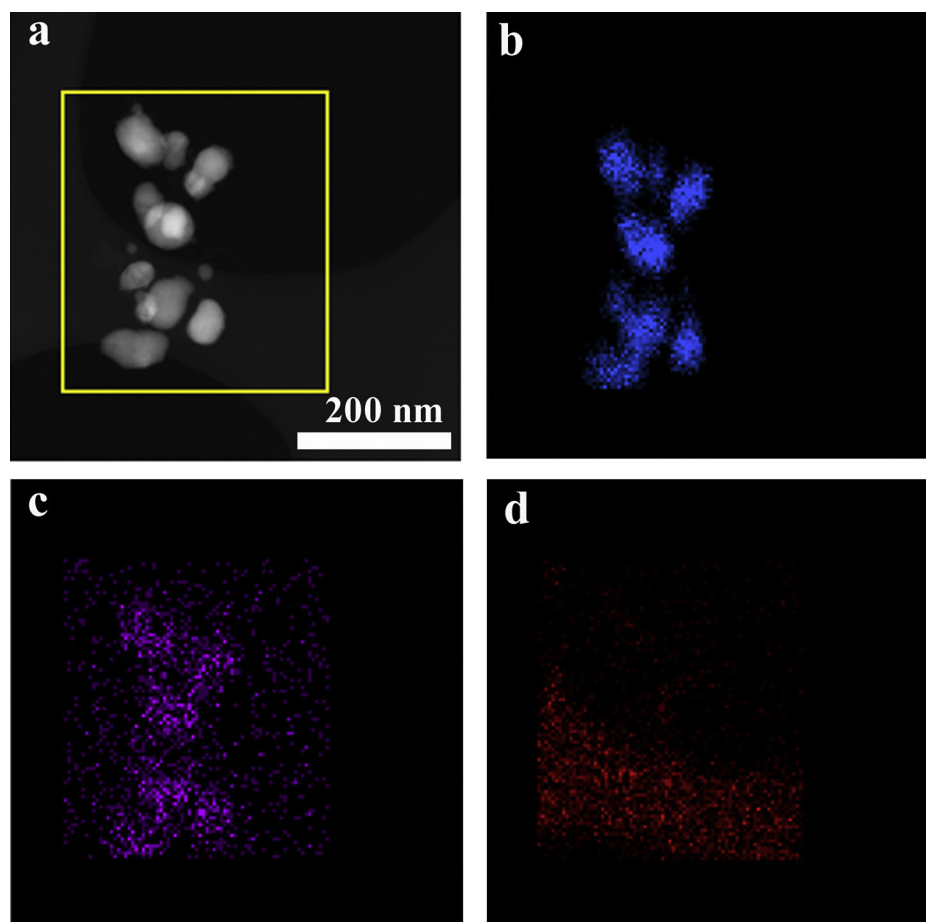


Fig. 2. TEM analysis of carbon-coated Cu-Co bimetallic catalyst (Cu:Co = 1:3). (a) TEM dark-field image; (b) Elemental mapping of cobalt; (c) Elemental mapping of copper; (d) Elemental mapping of carbon.

from VG Scientific using 300 W Al-K α radiations. The base pressure was approximately 3×10^{-9} mbar. The binding energies were referenced to the C1 s line at 284.8 eV from adventitious carbon. The Eclipse V2.1 data analysis software supplied by the VG ESCA-Lab200I-XL instrument manufacturer was used to manipulate the acquired spectra.

2.4. Catalytic activity test

For a typical run, to a 50-mL autoclave with Teflon liner were added 5-hydroxymethylfurfural (0.25 g), catalyst (20 mg), and absolute ethanol (10 ml). The autoclave was sealed and purged with H₂ several times. The hydrogenolysis reaction was performed at given temperature and hydrogen pressure under stirring. After the reaction, product/catalyst separation was performed by simple filtration. In consecutive batch tests, continuous filtration was applied to separate the catalyst. The catalyst was recycled into the autoclave with the feedstock stream.

The products were analyzed by GC and GC–MS. GC was performed by using a GC-2014 instrument (Shimadzu) with a high-temperature capillary column (MXT-1, 30 m, 0.25 mm ID) and flame ionization detector (FID). The conversion and selectivity values were determined by GC with toluene as the internal standard. GC–MS is used to confirm chemical structures of the components in the product mixtures. GC–MS was performed by using a GCT Premier instrument (Waters) with a capillary column (DB-5MS/J&W Scientific, 30 m, 0.25 mm ID).

3. Results and discussions

3.1. Preparation and characterization of carbon coated bimetallic nanoparticles

Under solvothermal reaction conditions, the precursors are formed in the presence of tartaric acid and polyethylene glycol from metal ions. Polyethylene glycol is the carbon source for carbon layer developed in the further heating treatment. Another role of this polymer is the reductant for the formation of bimetallic nanoparticles. Carbon-coated Cu-Co bimetallic nanoparticles are in the size range from 10 nm to 60 nm (Fig. 1a). The average particle size is about 30 nm. Carbon layers over the bimetallic nanoparticles are clearly revealed by close views of TEM (Fig. 1c and d). The thickness of carbon shell is in the range from 2 to 6 nm. These graphene-like layers provide protection against oxidation and deactivation. In order to investigate the elemental composition and the distribution of the element in the composite catalysts, the energy-dispersive spectroscopy (EDS) elemental mapping analysis is conducted on the several particles in the marked areas (Fig. 2a). Every nanoparticle contains both Co and Cu, and Co and Cu are uniformly distributed in the particles (Fig. 2b, c). There are some copper signal noises outside the composite nanoparticles. This is attributed to copper mesh used as the sample support for TEM analysis. Elemental mapping of carbon also overlap the noise signals from carbon membrane of TEM sample support (Fig. 2d).

X-ray photoelectron spectroscopy (XPS) measurement is performed to investigate the chemical composition of carbon-coated Cu-Co bimetallic nanoparticles. XPS survey spectrum (Fig. 3a)

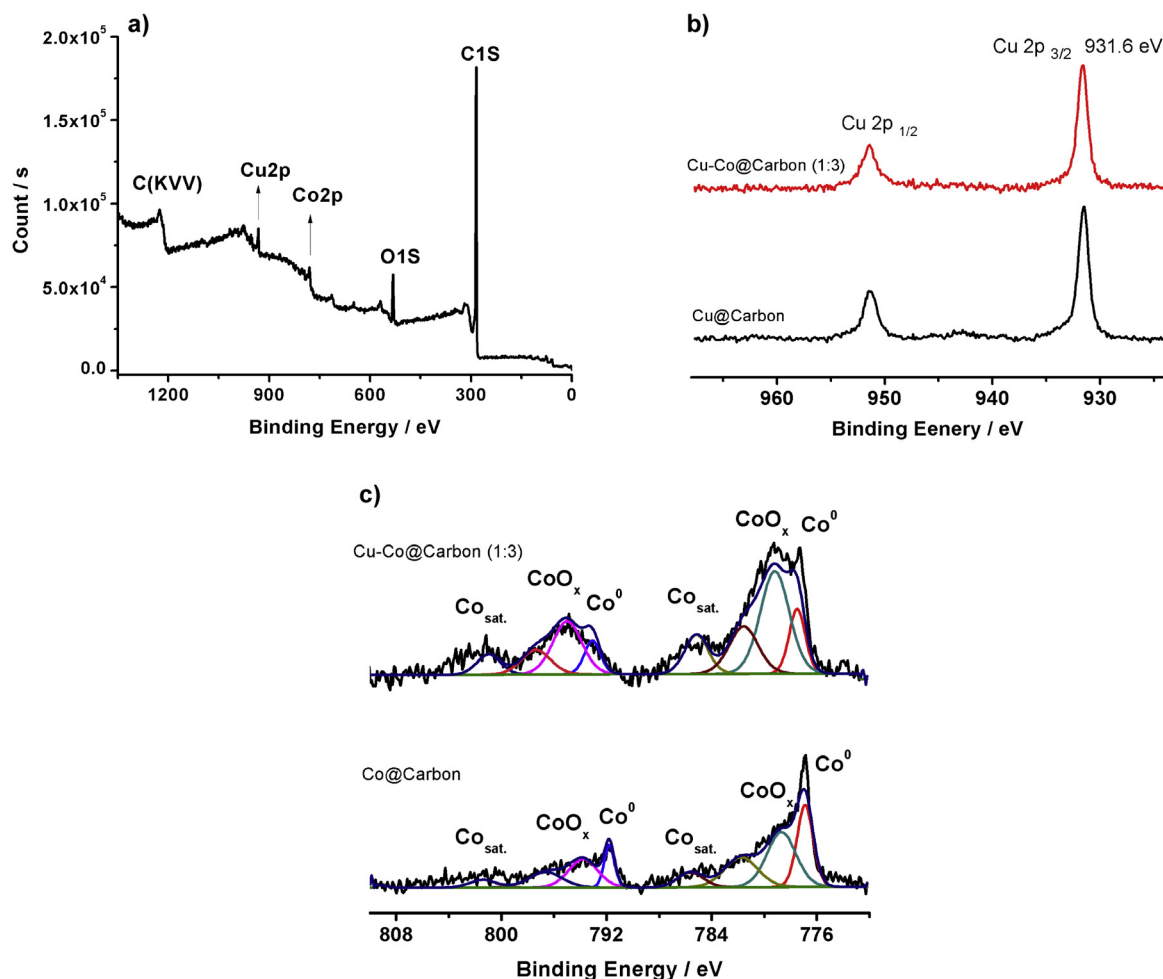


Fig. 3. (a) XPS survey spectrum of carbon-coated Cu-Co bimetallic catalyst (Cu:Co = 1:3). (b) Fitting of Cu 2p envelopes. (c) Fitting of Co 2p envelopes.

reveals the presence of copper, cobalt, carbon and oxygen. Cu $2p_{3/2}$ and $2p_{1/2}$ XPS peaks are at the binding energy values of 931.6 eV and 951.4 eV (Fig. 3b). The single metal sample (Cu@Carbon) prepared by the same method shows similar XPS peaks of Cu 2p. These indicate that copper species are in the zero-valent states [43]. Co 2p XPS peaks show more complex patterns (Fig. 3c). Fitting of the Co 2p envelope leads to the identification of three patterns: zero-valent metal species (Co $2p_{1/2}$ 777.5 eV) [44], cobalt oxide species (Co $2p_{1/2}$ 781.6 eV) [45,46], and the shakeup satellite signals (785.2 eV and 801.0 eV) [47]. The single metal sample (Co@Carbon) shows the same trend. However, zero-valent cobalt species have a higher atomic concentration.

As revealed by powder X-ray diffraction patterns (Fig. 4a), the diffraction lines of Co (111), (200), and (220) (PDF#15-0806) are observed at 44.2° , 51.5° , and 75.8° for carbon-coated cobalt nanoparticles and the diffraction lines of Cu (111), (200), and (220) (PDF#04-0836) are detected at 43.2° , 50.4° , and 74.1° for carbon-coated copper nanoparticles. The lines characteristic of carbon layers ($2\theta = 26.4^\circ$) (PDF#41-1487) were detected in all samples. For the bimetallic catalysts, when the mole ratio of Cu to Co was changed from 3:1 to 1:5, the diffraction intensity of copper peaks decreases and that of cobalt peaks increases (Fig. 4b). Bimetallic catalysts with various components are further characterized by powder XRD (Fig. 4c and d). The main lines characteristic of Ag(111), (200), (220) and (311) are observed at (38.1°) , (44.2°) , (64.4°) and (77.4°) in the Ag-Co@C catalysts (PDF# 04-0783). No significant diffraction lines of Zn and Ni species are detected. The diffraction lines of Ni (111), (200), (220) (PDF# 04-0850) are observed

at $2\theta = 44.5^\circ$, 51.7° , and 76.3° . Fe(110), and (200) (PDF#06-0696) are detected at 44.6° and 65.0° . The diffraction lines of ZnO are clearly observed at 31.6° , 34.3° and 36.1° (PDF# 36-1451) in the XRD patterns of Cu-Zn@C catalyst.

3.2. Hydrogenolysis of HMF to DMF

The conversion of HMF to DMF involves two main steps: the hydrogenation of the aldehyde groups and the subsequent hydrogenolysis of hydroxymethyl groups. There are many side products during the conversion, such as ring hydrogenation and ring-opening product, as shown in Scheme 1. The conversion of HMF to DMF over Cu-Co(1:3)@Carbon is performed in ethanol at 180°C under the hydrogen pressure of 5.0 MPa. HMF is totally converted and the catalytic process gives a very high selectivity of DMF (99.4%).

Fig. 5a shows the effect of reaction temperature on the catalytic performance of carbon-coated Cu-Co bimetallic catalysts. At relatively low reaction temperature (140°C), the HMF conversion is 64.2% and the selectivity of DMF is 55.5%. The main byproducts are tetrahydrofuran (THF) (23.3%) and ring-opening product hexane-2, 5-diol (HDL) (15%). Ring-opening product is from the isomerization of the low temperature hydrogenation product (DHMF). When the temperature increases to 200°C , HMF is totally converted. However, the selectivity of DMF is only 33.7% and THF is the main product (65.4%). Other byproducts, such as decarbonylation products (5-methylfuran-2-yl) methanol (MFA) and ring-opening product hexane-2, 5-diol (HDL), were also detected

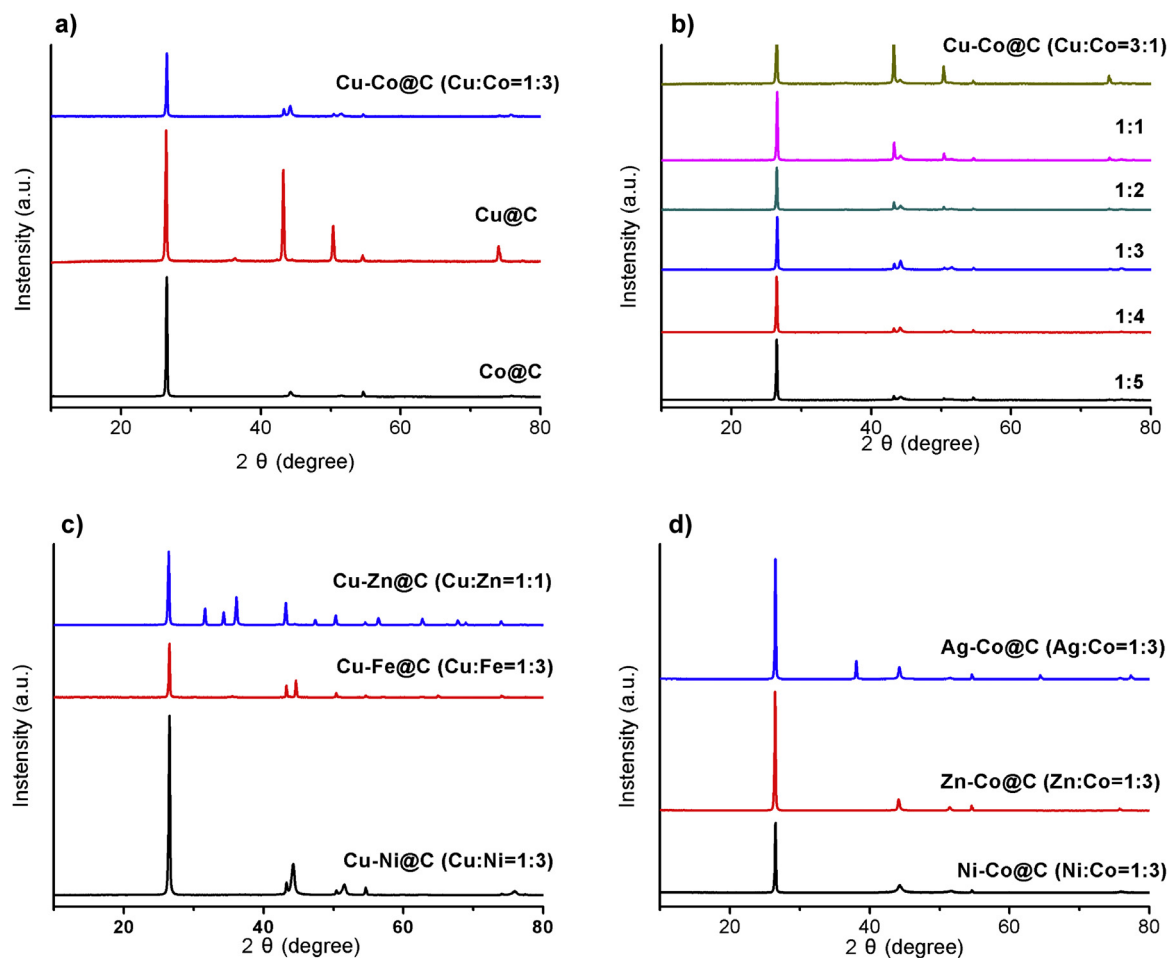
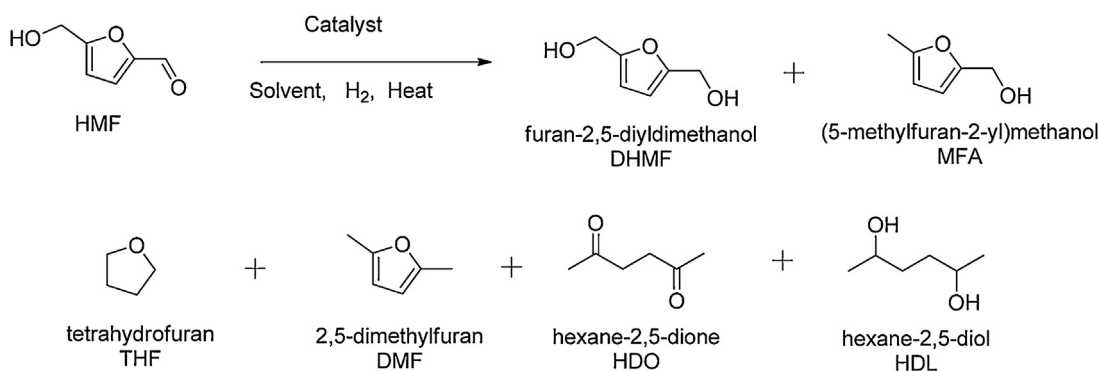


Fig. 4. (a) Powder XRD patterns of carbon-coated Cu-Co bimetallic catalyst (Cu:Co = 1:3) and related single metal samples. (b) Powder XRD patterns of carbon-coated Cu-Co bimetallic catalysts with various proportions. (c) Powder XRD patterns of carbon-coated Cu based bimetallic catalysts. (d) Powder XRD patterns of carbon-coated other Co based bimetallic catalyst.



Scheme 1. Possible products during hydrotreating HMF.

in the reaction mixture. The conversion of HMF to DMF over Cu-Co (1:3)@Carbon can give a total conversion of HMF after six-hour reaction. After 10 h, the selectivity of DMF decreases to 94.1%. Three types of solvents are selected as the reaction medium (Fig. 5b), including alcohols (ethanol, *n*-propanol, and *i*-propanol), ether (tetrahydrofuran (THF) and cyclopentyl methyl ether (CPME)), and nonpolar hydrocarbon (toluene). Alcohols are the most suitable reaction medium. The yield of DMF is 99.4% in ethanol, 94% in *n*-propanol, and 98.3% in *i*-propanol. Toluene is a poor solvent for HMF hydrogenolysis. The yield of DMF is only 67.8% with total conversion of HMF. Hydrogen pressure shows a slight impact

on the catalytic performance (Fig. 5c). The best result (99.4%) is obtained at hydrogen pressure of 5 MPa. The DMF yield shows a little decrease (96.9%) at 6 MPa. Low reaction pressure is unfavorable to the hydrogenolysis of hydroxymethyl of furan ring, but the higher reaction pressure may lead to total hydrogenation and ring-opening of furan.

Carbon-coated Cu-Co bimetallic nanocatalysts with different proportions of metal species are further screened in catalytic activity tests (Table 1). Two single metal catalysts (Cu@Carbon and Co@Carbon) are selected as control subjects. The reaction over Cu@Carbon gives a HMF conversion of 70%. Partial hydrogenation

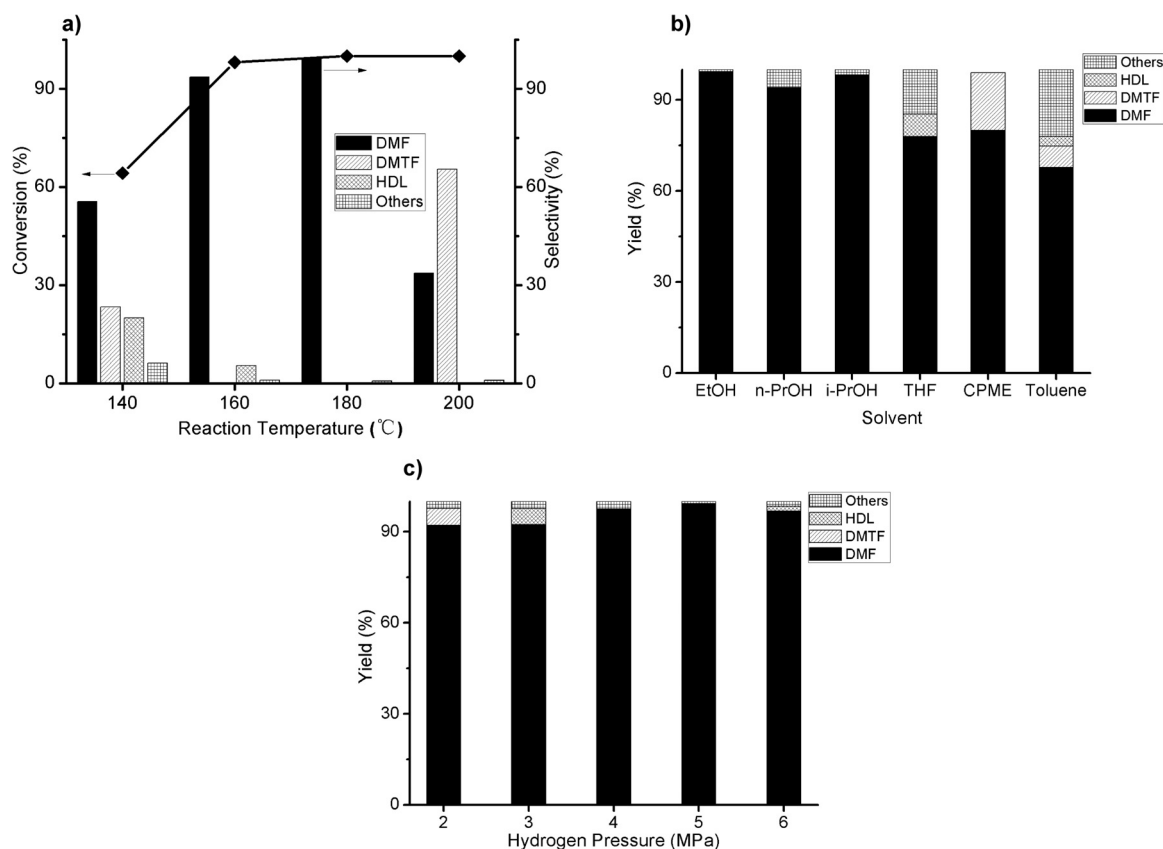
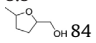


Fig. 5. (a) The influence of reaction temperature on catalytic performance over carbon-coated Cu-Co bimetallic catalyst (Cu:Co = 1:3). (b) The influence of reaction solvent on catalytic performance over carbon-coated Cu-Co bimetallic catalyst (Cu:Co = 1:3). (c) The influence of hydrogen pressure on catalytic performance over carbon-coated Cu-Co bimetallic catalyst (Cu:Co = 1:3).

Table 1

Screening results of the hydrogenolysis of HMF over Cu-Co@Carbon catalysts with different compositions.

Entry	Catalyst	Selectivity (%)					Conversion (%)
		DMF	THF	HDL	DHMF	Others	
1	Cu-Co@C (Cu:Co = 3:1)	77.6	8.9	13.5	–	–	93.7
2	Cu-Co@C (Cu:Co = 1:1)	83.2	11.9	–	–	4.9	100
3	Cu-Co@C (Cu:Co = 1:2)	94.8	–	–	–	5.2	100
4	Cu-Co@C (Cu:Co = 1:3)	99.4	–	–	–	0.6	100
5	Cu-Co@C (Cu:Co = 1:4)	98.8	–	–	–	1.2	100
6	Cu-Co@C (Cu:Co = 1:5)	99.1	–	–	–	0.9	100
7	Cu@C	10.8	8.5	–	76.8	3.90	70.0
8	Co@C	91.9	–	–	–	8.1	100
9	Cu@C & Co@C	91.2	–	–	–	8.8	100
10	Co/AC ^a	2.1	13.9	–	–		100

Reaction conditions: to a 50-mL autoclave were added 0.25 g HMF/10 ml ethanol, 20 mg catalyst. Hydrogen: 5.0 MPa, temperature: 180 °C, reaction time: 8.0 h. Conversions and selectivity were determined by GC with toluene as the internal standard.

^a Cobalt supported over activated carbon. Reduced by hydrogen flow over 400 °C.

molecule (DHMF) is the main product (76.8%) and the selectivity of DMF is 10.8%. Co@Carbon is a relatively efficient catalyst for hydrogenolysis of HMF. The selectivity of DMF is achieved with the HMF conversion of 100%. The physical mixture of Cu@Carbon and Co@Carbon shows catalytic performance similar to Co@Carbon. No bimetallic synergistic effects are observed in this case. Co/AC is reduced by hydrogen flow over 400 °C. The reduced cobalt species cannot be kept stable and oxidation is inevitable. As shown by entry 10 of Table 1, the total hydrogenation of HMF is the main reaction over Co/AC. The selectivity of DMF is very low. The promoting roles of CoO_x species in the hydrogenolysis of hydroxyl groups have been reported in the hydrogenolysis of HMF over the Ru/Co₃O₄ catalyst [15]. The best result is obtained over the catalyst with the

mole ratio of 1/3 (Cu/Co). The selectivity of DMF increases to 99.4% based on the synergistic effect between copper and cobalt species. As revealed by XPS measurement (Fig. 3c), cobalt species are partially reduced to zero-valent cobalt. The coexistence of cobalt oxide species endows the supported nanoparticles with high selectivity and activity in the integrated hydrotreating of HMF to DMF. Copper species show very low selectivity of DMF (10.8%), however, they can improve the catalytic performance of cobalt species.

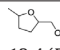
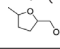
Bimetallic nanocatalysts with various compositions are prepared through the same method as Cu-Co@Carbon. There are two types of catalysts: cobalt-based catalysts and copper-based catalysts. Their catalytic activity data are summarized in Table 2. Cobalt-based catalysts show high activity in converting HMF to

Table 2
Screening results of the hydrogenolysis of HMF over different bimetallic catalysts.

Entry	Catalyst	Selectivity (%)					Conversion (%)
		DMF	THF	HDL	DHMF	Others	
1	Cu-Co@C (Cu:Co = 1:3)	99.4	–	–	–	0.6	100
2	Ni-Co@C (Ni:Co = 1:3)	97.8	–	–	–	2.2	100
3	Zn-Co@C (Zn:Co = 1:3)	91.5	–	7.6	–	0.9	100
4	Ag-Co@C (Ag:Co = 1:3)	96.2	–	1.8	–	2.0	100
5	Cu-Ni@C (Cu:Ni = 1:3)	86.7	–	–	–	13.3	22.8
6	Cu-Fe@C (Cu:Fe = 1:3)	4.4	88.5	–	7.1	–	91.0
7	Cu-Zn@C (Cu:Zn = 1:1)	4.0	–	–	82.9	13.05	63.9

Reaction conditions: to a 50-mL autoclave were added 0.25 g HMF/10 ml ethanol, 20 mg catalyst. Hydrogen: 5.0 MPa, temperature: 180 °C, reaction time: 8.0 h. Conversions and selectivity were determined by GC with toluene as the internal standard.

Table 3
Catalytic hydrogenolysis of HMF over commercial available noble metal catalysts over activated carbon.

Entry	Catalysts	Conversion (%)	Selectivity (%)			
			DMF	THF	HDL	Others
1	Pd/C (10 wt%)	100	6.93	–	–	 91, 2.1 (others)
2	Ru/C (5 wt%)	65.6	86.6	–	–	13.4 (DHMF)
3	Rh/C (5 wt%)	97.9	78.8	–	7.1	14.1
4	Pt/C (5 wt%)	66.1	71.0	–	–	11.7 (DHMF), 17.2 (others)
5	Raney Ni	100	0.9	18.9	–	 80.2 80.2

Reaction conditions: to a 50-mL autoclave were added 0.25 g HMF/10 ml ethanol, 20 mg catalyst. Hydrogen: 5.0 MPa, temperature: 180 °C, reaction time: 8.0 h. Conversions and selectivity were determined by GC with toluene as the internal standard.

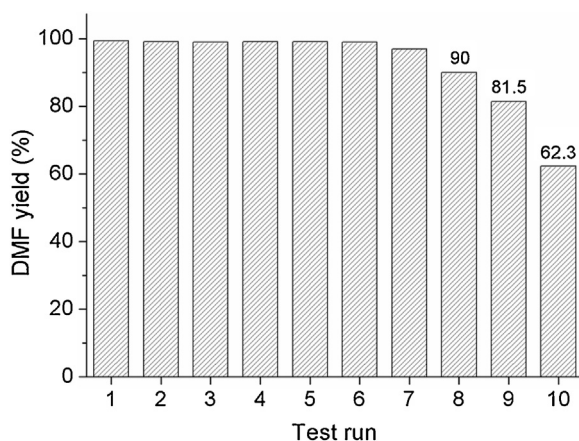


Fig. 6. Ten-run recycling test of carbon-coated Cu-Co bimetallic catalyst (Cu:Co = 1:3).

DMF. Copper-based catalysts have relatively poor catalytic performance. Several commercial hydrotreating catalysts are tested as benchmark data to evaluate the catalytic performance of Cu-Co (1:3) @Carbon (Table 3). Rh/C is the most active catalyst. HMF is totally converted and the selectivity of DMF reaches 78.8%. Ru/C and Pt/C show moderate performances. The conversions over Pd/C and Raney Ni give (5-methyltetrahydrofuran-2-yl) methanol (MTHFL) as the main products. These results reveal that the as-synthesized Cu-Co@Carbon catalysts exhibit better catalytic performances in hydrotreating HMF to DMF than those of commercial noble catalysts.

3.3. Recyclability of Cu-Co@Carbon during hydrogenolysis of HMF

The recyclability of Cu-Co@Carbon bimetallic catalyst is investigated through a ten-run recycling test of HMF hydrogenolysis (Fig. 6). After the ninth recycling batch, there is a loss in the DMF yield. In the tenth test, the deactivation is observed and the DMF yield decreases to 62.3%. As revealed by XPS measurement,

the loss of catalytic activity is related to the gradual oxidation of active metallic cobalt species (Fig. 7a). Carbon layers over bimetallic nanoparticles are gradually abraded by the inevitable intergranular friction, the collision with the stirrer and autoclave wall, and the leaching effect of the solvent (Fig. 7b, c). The vanishment of protection coating directly leads to oxidation of active metallic cobalt species. Carbon layers should be kept in appropriate thickness to balance protection coating and surface accessibility to the reactant molecules. Bimetallic nanoparticles can be over-loaded with carbon layers through treatment at elevation of temperature (1000 °C) and the resulting materials show relatively poor catalytic activity. The introduction of copper species can improve the recyclability of the Cu-Co@Carbon bimetallic catalyst. In the control experiment, a single metal catalyst of cobalt can only be recycled for three times. HMF is a thermal polymerization molecule. Under reaction conditions, part of the reactants can be polymerized (less than 9%). With the accumulation of polymerization products, the Co catalyst gradually loses its activity (after three-batch recycling). The function role of copper species is to avoid the accumulation of polymerization products and leads to good recyclability of Cu-Co bimetallic catalyst.

4. Conclusion

In summary, carbon coated Cu-Co bimetallic nanoparticles (Cu-Co@Carbon) were prepared through heating treatment of the bimetallic oxide precursors. Polyethylene glycol over the precursors acts as the carbon sources of carbon layers and the reductant for metal species. The simultaneous formation of carbon layers over the nanoparticles protects them from oxidation and deactivation. The Cu-Co@Carbon catalyst shows excellent performance in selective hydrogenolysis of HMF to DMF. The yield of DMF reaches approximately 99.4% and exceeds the results of supported noble metal catalysts. The catalyst show good recyclability and recoverability in a six-run recycling test. This work provides a novel and insightful strategy to develop low-cost and high-performance hydrotreating catalysts based on base metals for industrial organic process and valorization of renewable biomass.

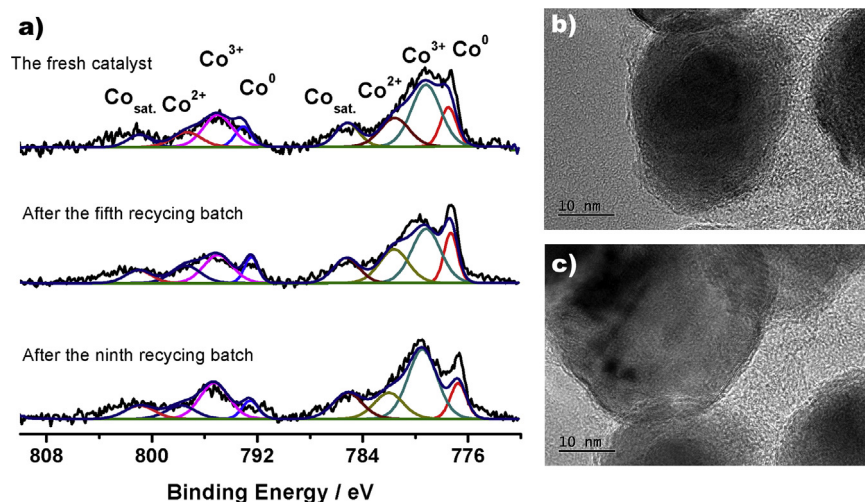


Fig. 7. (a) Fitting of Co 2p envelopes of the fresh catalyst and the used catalysts. (b) TEM image of the carbon-coated Cu-Co bimetallic catalyst (Cu:Co = 1:3) after the fifth recycling batch. (c) TEM image of the carbon-coated Cu-Co bimetallic catalyst (Cu:Co = 1:3) after the ninth recycling batch.

Acknowledgement

This work was financially supported by the National Natural Sciences Foundation of China (nos. 21403248, 21174148, 21101161, 21304101).

Reference:

- [1] G.W. Huber, S. Iborra, A. Corma, *Chem. Rev.* 106 (2006) 4044–4098.
- [2] J.C. Serrano-Ruiz, R. Luque, A. Sepulveda-Escribano, *Chem. Soc. Rev.* 40 (2011) 5266–5281.
- [3] T. Thananattathanachon, T.B. Rauchfuss, *Angew. Chem. Int. Ed.* 49 (2010) 6616–6618.
- [4] Y. Roman-Leshkov, C.J. Barrett, Z.Y. Liu, J.A. Dumesic, *Nature* 447 (2007) 982–985.
- [5] J.P. Lange, E. van der Heide, J. van Buijtenen, R. Price, *ChemSusChem* 5 (2012) 150–166.
- [6] K. Yan, T. Lafleur, X. Wu, J. Chai, G. Wu, X. Xie, *Chem. Commun.* 51 (2015) 6984–6987.
- [7] R.J. van Putten, J.C. van der Waal, E. de Jong, C.B. Rasrendra, H.J. Heeres, J.G. de Vries, *Chem. Rev.* 113 (2013) 1499–1597.
- [8] B. Saha, M.M. Abu-Omar, *ChemSusChem* 8 (2015) 1133–1142.
- [9] W. Yang, A. Sen, *ChemSusChem* 4 (2011) 349–352.
- [10] N. Nikbin, S.T. Feng, S. Caratzoulas, D.G. Vlachos, *J. Phys. Chem. C* 118 (2014) 24415–24424.
- [11] R. Xiong, S.I. Sandler, D.G. Vlachos, P.J. Dauenhauer, *Green Chem.* 16 (2014) 4086–4091.
- [12] J.J. Bozell, G.R. Petersen, *Green Chem.* 12 (2010) 539–554.
- [13] Y. Nakagawa, M. Tamura, K. Tomishige, *ACS Catal.* 3 (2013) 2655–2668.
- [14] B. Saha, C.M. Bohn, M.M. Abu-Omar, *ChemSusChem* 7 (2014) 3095–3101.
- [15] Y. Zu, P. Yang, J. Wang, X. Liu, J. Ren, G. Lu, Y. Wang, *Appl. Catal. B* 146 (2014) 244–248.
- [16] G. Wang, J. Hilgert, F.H. Richter, F. Wang, H.J. Bongard, B. Spliethoff, C. Weidenthaler, F. Schüth, *Nat. Mater.* 13 (2014) 293–300.
- [17] D. Scholz, C. Aellig, I. Hermans, *ChemSusChem* 7 (2014) 268–275.
- [18] J. Jae, W.Q. Zheng, R.F. Lobo, D.G. Vlachos, *ChemSusChem* 6 (2013) 1158–1162.
- [19] D.J. Cole-Hamilton, *Science* 299 (2003) 1702–1706.
- [20] D.J. Cole-Hamilton, R.P. Tooze, *Catalyst Separation, Recovery and Recycling: Chemistry and Process Design*, Springer, Dordrecht, 2006.
- [21] B. Cornils, W.A. Herrmann, I.T. Horvath, W. Leitner, S. Mecking, H. Olivier-Borbigou, D. Vogt, *Multiphase Homogeneous Catalysis*, Wiley, Weinheim, 2005.
- [22] M. Benaglia, *Recoverable and Recyclable Catalysts*, Wiley-Blackwell, Chichester, 2009.
- [23] A. Corma, H. Garcia, F.X.L. Xamena, *Chem. Rev.* 110 (2010) 4606–4655.
- [24] S. Ogasawara, S. Kato, *J. Am. Chem. Soc.* 132 (2010) 4608–4613.
- [25] H.E. Schoemaker, D. Mink, M.G. Wubbolds, *Science* 299 (2003) 1694–1697.
- [26] C. Ellis, *Hydrogenation of Organic Substances*, 3rd ed., Van Nostrand, New York, 1930, pp. 112–156.
- [27] R. Schroter, *Angew. Chem.* 54 (1941) 229–234.
- [28] E. Lieber, F.L. Morritz, *Adv. Catal.* 5 (1953), 417–255.
- [29] H. Adkins, H.R. Billica, *J. Am. Chem. Soc.* 70 (1948) 695–698.
- [30] J.H. Long, J.C.W. Frazer, E. Ott, *J. Am. Chem. Soc.* 56 (1934) 1101–1106.
- [31] P.H. Emmett, N. Skau, *J. Am. Chem. Soc.* 65 (1943) 1029–1035.
- [32] V.N. Ipatieff, B.B. Corson, I.D. Kurbatov, *J. Phys. Chem.* 43 (1939) 589–604.
- [33] A.F. Thompson Jr., S.B. Wyatt, *J. Am. Chem. Soc.* 62 (1940) 2555–2556.
- [34] M.R. Friedfield, *Science* 342 (2013) 1076–1080.
- [35] H.M.T. Galyis, *Science* 335 (2012) 835–838.
- [36] F.A. Westerhaus, R.V. Jagadeesh, G. Wienhofer, M.M. Pohl, J. Radnik, A.E. Surkus, J. Rabeah, K. Junge, H. Junge, M. Nielsen, A. Bruckner, M. Beller, *Nat. Chem.* 5 (2013) 537–543.
- [37] V.R. Calderone, N.R. Shiju, D. Curulla-Ferr, S. Chambrey, A. Khodakov, A. Rose, J. Thiessen, A. Jess, G. Rothenberg, *Angew. Chem. Int. Ed.* 52 (2013) 4397–4401.
- [38] R.D.L. Smith, M.S. Preivot, R.D. Fagan, S. Trudel, C.P. Berlinguette, *J. Am. Chem. Soc.* 135 (2013) 11580–11586.
- [39] Y. Huang, M. Chen, L. Yan, Q. Guo, Y. Fu, *ChemSusChem* 7 (2014) 1068–1070.
- [40] A.J. Kumalaputri, G. Bottari, P.M. Erne, H.J. Heeres, K. Barta, *ChemSusChem* 7 (2014) 2266–2275.
- [41] L. Yu, L. He, J. Chen, J. Zheng, L. Ye, H. Lin, Y. Yuan, *ChemCatChem* 7 (2015) 1701–1707.
- [42] G. Bottari, A.J. Kumalaputri, K.K. Krawczyk, B.L. Feringa, H.J. Heeres, K. Barta, *ChemSusChem* 8 (2015) 1323–1327.
- [43] K.L. Deutsch, B.H. Shanks, *J. Catal.* 285 (2012) 235–241.
- [44] J. Long, Y. Zhou, Y. Li, *Chem. Commun.* 51 (2015) 2331–2334.
- [45] H. Yang, H. Dai, J. Deng, S. Xie, W. Han, W. Tan, Y. Jiang, C.T. Au, *ChemSusChem* 7 (2014) 1745–1754.
- [46] B. Bai, J. Li, *ACS Catal.* 4 (2014) 2753–2762.
- [47] C. Jia, M. Schwickardi, C. Weidenthaler, W. Schmidt, S. Korhonen, B.M. Weckhuysen, F. Schuth, *J. Am. Chem. Soc.* 133 (2011) 11279–11288.